Journal of Marine Science and Technology, Vol. 25, No. 4, pp. 435-441 (2017)
DOI: 10.6119/JMST-017-0329-1

AN IMPROVED ALGORITHM OF TRUBULENCE SIGNAL DENOISING BASED ON LMS ADAPTIVE FILTERING

Xue Chen[1], Da-lei Song[2], Xin Luan[1], Hua Yang[1], and Xiu-yan Liu[1]

Key words: ocean turbulence, dissipation rate of TKE, denoising, LMS adaptive filter.

ABSTRACT

Restricted by observation instruments and methods, the measured turbulence signals in the open ocean are inevitably affected by noise. To maximum eliminate the noise caused by the vibration of the instruments and improve the accuracy of the measured turbulence signals, an improved turbulence signal denoising algorithm based on least mean square (LMS) adaptive filter is proposed in this paper. The key point of the improved algorithm is to obtain the optimal weight value by the adaptive adjustment and remove the vibration noise from the measured shear signals in frequency domain. Through taking the Nasmyth theoretical spectrum as the desired signal to update the weight value, we can obtain the optimal estimation of the observation spectrum, especially at the shedding frequency. Sea data obtained from a moored turbulence measuring instrument (MTMI) deployed in the South China Sea is used to verify the feasibility and validity of the improved algorithm. The results show that the corrected spectra agree well with the Nasmyth theoretical spectra and the calculated dissipation rates of turbulent kinetic energy (TKE) drop near an order of magnitude compared with the raw measured data, which indicate that the improved turbulence denoising algorithm can effectively eliminate the vibration noise and provide accurate data for studying the characteristics of turbulence mixing.

I. INTRODUCTION

Turbulence mixing is one of the main physical processes that control the ocean overturning circulation at a wide range of temporal and spatial scales because of its influences on climate. At small scales, turbulence affects the ocean circulation and ecosystems by enhancing the transport of heat and nutrients within the water column. The ocean turbulence has become an important subject in the marine science research (Fer and Paskyabi, 2013).

Conventionally, ocean turbulence is measured by shear probes and/or fast response thermistors, sampling the dissipation subrange of the turbulence spectrum. However, to measure a few centimeters of turbulence microstructure in the open sea is quite difficult due to its inherent characteristics of chaotic, unsteady and unpredictable. Noise is inevitable in the actual turbulence observation process and it mainly includes natural noise (usually due to the probes encountering plankton or other detritus in the water column), vehicle motion and vibration, and the high frequency electronic system noise (Lueck et al., 1997). The noise distributes at different frequency bands and leads to different effects on the observed signals. As an advanced turbulence observation platform, the mooring system can meet the requirements of long time and fixed-point ocean turbulence measurement. However, this kind of observation platform is susceptible to vortex-induced vibration at the shedding frequency, which may lead to the error estimation of the dissipation rate of turbulent kinetic energy (TKE). So, the noise caused by vibration should be removed from the measured turbulence shear signals to acquire high-precision data.

To get rid of the noise, many methods have been proposed, such as low-pass filter based on Fourier transform, the spatial power-response transfer function (Lueck et al., 1977). These methods aim at removing the contamination in the high frequency and have no denoising effect on removing the vibration noise distributed in the low frequency. Cross-spectrum denoising method (Goodman et al., 2006) is proposed to remove the noise caused by the instrument vibration. Through calculating the weight value, the coherence of the measured shear related to the detected acceleration can be obtained and the vibration noise can be eliminated at some extent. However, this denoising method treats all the wavenumbers as the same and lacks the optimal estimation of the weight value, so, the obtained corrected spectrum is not the optimal state.

As an advanced signal processing technology, LMS adaptive filter is widely used in effective signals extraction, such as eliminate the noise in the communication system and extract the

Paper submitted 06/23/16; revised 09/12/16; accepted 03/29/17. Author for correspondence: Hua Yang (e-mail: hyang@ouc.edu.cn).
[1] College of Information Science and Technology, Ocean University of China, Qingdao, China.
[2] College of Engineering, Ocean University of China, Qingdao, China.

effective signals from strong background noise (Dixit and Nagaria, 2016), vehicle vibration signal denoising (Zhang et al., 2013). In time domain, LMS adaptive filter has presented good performance in non-stationary signal analysis and processing (Widrow et al., 1976; Deborah et al., 2016). In the turbulence research, The quality of the observed velocity fluctuations signals are evaluated through comparing the observed wavenumber spectrum with an empirical spectrum that is used as standard spectrum and derived by Nasmyth. Furthermore, the dissipation rate of TKE as a key parameter to describe the turbulence characteristic is also calculated in wavenumber domain using the measured turbulence velocity fluctuations (Levine and Lueck, 1999; Lueck and Huang, 1999).

Based on the above analysis, an improved turbulence denoising algorithm based on LMS adaptive filter is proposed and designed to conduct in frequency domain, which can achieve the optimal estimation of the observation spectrum and the dissipation rate of TKE. Through taking the Nasmyth theoretical spectrum as the desired signal, we can obtain more accurate estimation of the error function than traditional denoising in time domain. In addition, the weight value adaptively adjusts at different wavenumbers, which can more effectively eliminate the vibration noise at the shedding frequency. The sea data collected in the South China Sea with a moored turbulence measuring instrument (MTMI) is used to evaluate the validity of the improved turbulence denoising method.

The outline of this paper is as follows. The turbulence observation and the correlation of the measured signals are introduced in Section 2. Section 3 mainly presents the improved turbulence denoising algorithm based on LMS adaptive filter in detail and gives the process to calculate the TKE dissipation rate. Sea data results to verify the validity of the improved denoising algorithm are shown and discussed in Section 4 and conclusion remarks are finally given in Section 5.

II. TURBULENCE OBSERVATION AND PROCESS ANALYSIS

1. Deployment

The sea data used to verify the validity of the turbulence denoising algorithm is collected in the South China Sea (21°09.900′N 117°42.031′E) with a moored turbulence measuring instrument (MTMI) designed by OUC. In this experiment, the instrument had been deployed in about 250-m-deep water, and it successfully collected turbulence data for 110 days. The collected data includes shear voltage data, platform vibration data and attitude data, which lays the foundation for further analysis of the turbulence characteristics of the South China Sea. Throughout the observation period, the instrument responded to the ambient currents and the speed of the current measured by the Aanderaa current meter RCM11 was ranging from 0.05 to 0.48 m/s.

The MTMI is designed to collect abundant turbulence data from deep sea for a long time at a fixed level. The core component of MTMI is the turbulent observing part, which contains two orthogonal shear probes and three orthogonal accelerometers. The shear probes embedded in the middle of the nose are used to measure the cross-stream velocity fluctuations. In the design of the instrument, one probe is oriented to sense horizontal velocity fluctuations (w) and the other responds to the athwartships velocity fluctuations (v). The voltage output of the shear probes are converted to shear ($\partial w/\partial x$, $\partial v/\partial x$) using the electronic constants, the sensitivity of the shear probes and the velocity perpendicular to the shear probes. The output voltage of the two shear probes were sampled at 1024 Hz, digitized by 16-bit A/D conversion and finally stored in the storage card. To monitor the status of the instrument under the seawater, three orthogonal accelerometers are housed in the instrument cabin by a right-hand cartesian coordinate, which can provide information on attitude by Heading (rotation around the z axis and ranging from -180° to 180°), Pitch (rotation around the y axis and ranging from -90° to 90°) and Roll (rotation around the x axis and ranging from -180° to 180°). Meanwhile, the accelerometers can measure the instrument vibration of the accelerations in three directions: x, which is along the instrument axis and is positive forward (denoted as Accx); y, which points athwartship positive to the starboard side (denoted as Accy); and z, which is directed positive upward (denoted as Accz). With the sampling frequency set to 120 Hz, the output signal were digitized with a 16-bit A/D converter and stored in the storage card. The observation platform has good characteristics of stability and flexibility of current direction tracking, which is described by Xin Luan (Luan et al., 2016).

2. Analysis of the Signals Correlation

The microstructure turbulence is detected by the shear probe. The shear probe consists of a piezoelectric ceramic beam that can sense the turbulence shear force and produce a charge in response to the force. When use the turbulence observation instrument installed with the shear probe to conduct measurement in the open sea environment, the vehicle motion and vibration may cause large effect on the shear force. Then the output charge of the shear probe responds to the shear force and combines the true environmental turbulence shear with the vibration noise. So, the shear signals measured by the shear probe are always polluted by the vehicle body motion and vibration and we should minimize the contamination of the shear signals in the post-processing. In this paper, we estimate the vehicular motions and vibrations with the signals collected by the accelerometers.

The accelerations measured by the accelerometers include an inertial component and a gravitational component. Thus, the inertial component of the signals (denoted as dynamic accelerations) used to describe the vibration of the instrument can be separated from the gravity signals with independent pitch and roll information:

$$\mathrm{Accz} = \hat{a}_z + g\cos\theta\cos\varphi \tag{1}$$

where the angles θ and φ are the vehicle pitch and roll, g is the

acceleration of gravity, and $\hat{a}_z$ is the vertical inertial acceleration in the body frame. Similarly, the signals from the axial and athwartship are

$$\text{Accx} = \hat{a}_x + g\sin\theta \text{ and } \text{Accy} = \hat{a}_y + g\sin\varphi \quad (2)$$

respectively.

The core of the denoising is to remove the contamination to the shear signals by subtracting all coherent signals from the dynamic accelerations.

We assume the measured shear signals consist of the true environmental turbulence shear plus the contribution measured by the accelerometers due to the body motion and vibration, which can be expressed as:

$$s = \hat{s} + h * a \quad (3)$$

where, $\hat{s}$ is the measured shear from the probe, s is the true uncontaminated environmental shear and a is the component of acceleration corresponding to the shear. The weight value h represents the "transfer" of accelerations into the shear signals and the asterisk (*) denotes a convolution. Also, we assume that vehicular motions and vibrations are statistically independent of the environmental turbulence ($\overline{\text{sa}} = 0$). According to the above definition, our objective is to obtain the portion of the measured shear that is not coherent with the measured accelerations.

III. METHODOLOGY

Real and effective turbulence signals are the basis to analyze turbulence mixing characteristics. So, separating the desired signals from the environment background noise is an important and common problem in turbulence signal processing. In this paper, we use the acceleration measurements to minimize the contamination of the shear probe measurements by vehicular motions and vibrations of the probe mounts.

We remove the vibration noise in the measured shear with the model expressed in Eq. (3). To take advantage of the signals' spectral shape to assess the noise, we transform the signals from time domain into Fourier transform domain:

$$S = \hat{S} + HA \quad (4)$$

where, the uppercase symbols represent the Fourier transforms of the corresponding lowercase symbols. In cross spectrum denoising method, the correlation between the shear signals and the acceleration signals is denoted by the cross-power spectral density function.

$$H = C_{\hat{s}a}(f)/C_{aa}(f) \quad (5)$$

where, f denotes the frequency and H is the frequency weight value (transfer function) relating the shear signals to the acceleration signals. $C_{\hat{s}a}(f)$ is the cross-spectrum of the contaminated signal $\hat{s}$ and signal a. $C_{\hat{s}a}(f)$ reflects the correlation between the two kinds of signals. The double subscript denotes the auto-spectrum.

Multiply Eq. (4) by its complex conjugate, ensemble average and use the fact that $\overline{\text{sa}} = 0$, then the cleaned spectrum is obtained according to the below equation (Goodman et al., 2006):

$$C_{ss}(f) = C_{\hat{s}\hat{s}}(f) - \left|H(f)\right|^2 C_{aa}(f) \quad (6)$$

After obtaining the weight value, the vibration noise coherent with the measured acceleration can be estimated through multiplying the acceleration frequency spectrum by the weight value (Eq. (6)). So, the frequency spectrum of the shear can be corrected.

In Eq. (5), the weight value has to be calculated at each sampling point in frequency domain. Based on the analysis of Section 2, the contamination caused by the accelerations are mainly concentrate on the shedding frequency. In this paper, we propose to use the denoising method based on LMS adaptive filter to remove the contamination in every 3-min burst.

Let the weight value of the first pair of spectra calculated according to Eq. (5) as the initial weight value H. As H represents the "transfer" of accelerations into the shear signals, so, the acceleration auto-spectrum multiplied by the weight value denotes all coherent signals of accelerations corresponding to the shear:

$$C_{\hat{a}\hat{a}}(f) = H^T C_{aa}(f) \quad (7)$$

We can obtain the true environmental shear spectrum by subtracting the noise component from the measured shear auto-spectrum:

$$C_{ss}(f) = C_{\hat{s}\hat{s}}(f) - C_{\hat{a}\hat{a}}(f) = C_{\hat{s}\hat{s}}(f) - H^T C_{aa}(f) \quad (8)$$

All theoretical work on turbulence is based on its spatial and wavenumber structure. So, the cleaned spectrum is converted from frequency domain into a space-series (wavenumber domain) by multiplying the speed of the sensor using the Taylor's frozen turbulence hypothesis (Fer and Paskyabi, 2013):

$$C_{ss}(k) = C_{ss}(f)U \quad (9)$$

where, f denotes the frequency, U is the speed of the sensor through the water, $k = f/U$ denotes the wavenumber. Typically, the Nasmyth theoretical spectrum is used as the standard spectrum to evaluate the quality of the observed spectrum. Through the comparison between the cleaned shear spectrum and the Nasmyth theoretical spectrum, we can obtain the difference between the two spectra, namely, the error function $e(k)$ in wavenumber domain. Using the Taylor's frozen turbulence hypothesis can transform the error function into frequency domain:

$$e(k) = C_{tt}(k) - C_{ss}(k) \tag{10}$$

$$e(f) = e(k)/U \tag{11}$$

where, $C_{tt}(k)$ is the Nasmyth theoretical spectrum in wavenumber domain and $e(f)$ denotes the error function in frequency domain.

According to the LMS adaptive theory, the weight value constantly adjusts with the increase of the iterative number based on the error function. The next weight value is the sum of the current weight value and the acceleration auto-spectrum multiplied by the error function (Widrow et al., 1976):

$$H_{M+1}(f) = H_M(f) + 2\mu e(f) C_{aa}(f) \tag{12}$$

where, μ is the adaptation constant controlling the rate of convergence of the adaptive filter and M is the iteration number. After the constant adjustment of the weight value, the cleaned spectrum approximately equals to the desired spectrum and the noise component is removed effectively.

Assuming isotropic turbulence, the dissipation rate of turbulent kinetic energy (TKE) for each segment is calculated with the corrected shear spectra using the spectral integration (Oakey, 1982; Wolk et al., 2002):

$$\varepsilon = 7.5\nu \overline{(\frac{\partial w}{\partial x})^2} = 7.5\nu \int_{k_1}^{k_2} \Psi(k) dk \tag{13}$$

where, ν is the kinematic viscosity, the overbar denotes a spatial average and $\Psi(k)$ uses the corrected shear spectra $C_{ss}(k)$. The lower integration limit k_1 is set to 1 cpm (circle per meter) and the upper limit k_2 is the Kolmogorov wavenumber that represents the upper limit of the effective signals.

The flow chart of the improved denoising algorithm to calculate the dissipation rate of TKE is shown in Fig. 1. Where, N denotes the first pair of the shear spectrum and the acceleration spectrum, M is the iteration number, which is set to 10 in this paper. To remove the vibration noise coherent with the accelerometers data, each 3-min burst is segmented into half-overlapping 4-s-long portions for spectral analysis. In the improved algorithm, from the second pair of spectra, we no longer calculate the weight value based on the cross-spectrum of the two signals. Through adjusting the weight value in the adaptive process, the noise component will be removed effectively and the output spectrum will be much closer to the desired spectrum.

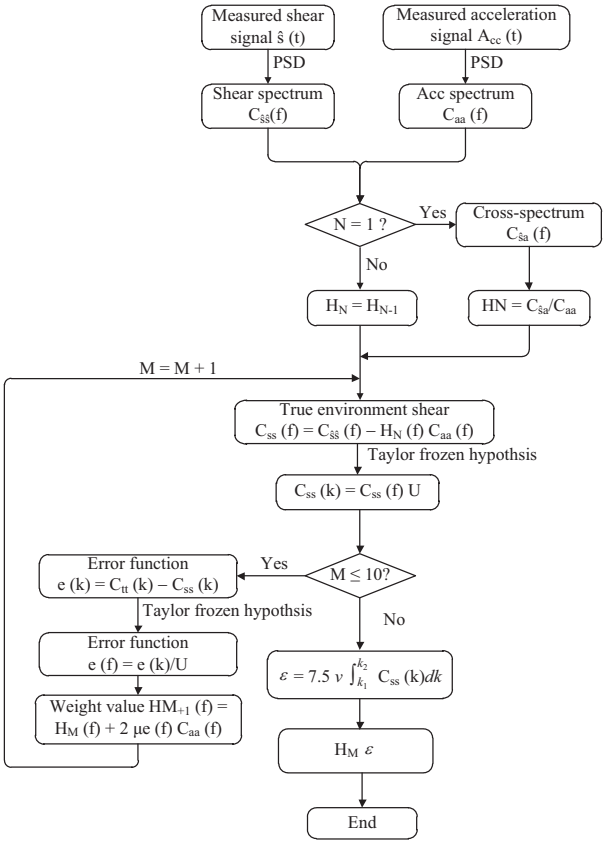

Fig. 1. Flow chart of the improved algorithm.

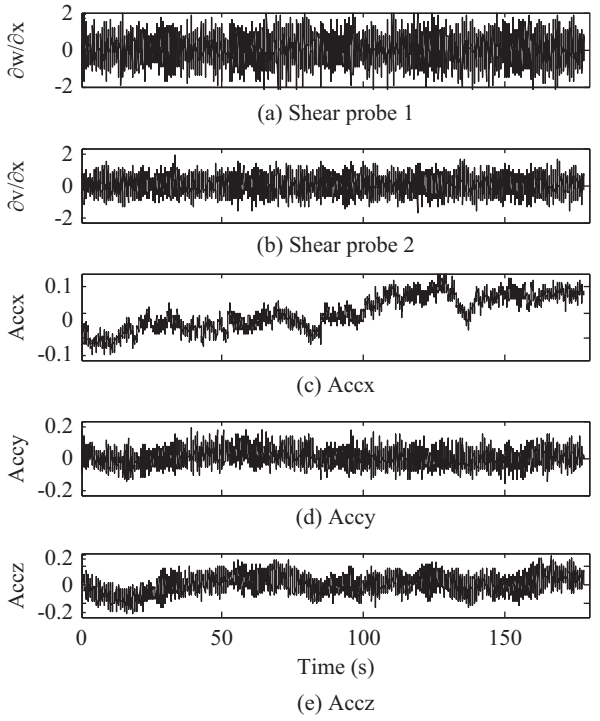

Fig. 2. Time series of the collected shear (s^{-1}) and accelerometer data from three-axis vibration sensors, Accx (m/s^2), Accy (m/s^2), and Accz (m/s^2), respectively, for a 3-min-long sample: (a) shear probe 1, (b) shear probe 2, (c) Accx, (d) Accy, and (e) Accz.

IV. RESULTS

In the filed test, the instrument collected abundant sea data from the deep sea for a long time at a fixed level. The shear signal sample processed in this paper is 3-min long and the corresponding velocity U = 0.26 m/s, which represents a 250-m velocity profile. The unprocessed shear signal sample contains contamination from the instrument motions and vibrations,

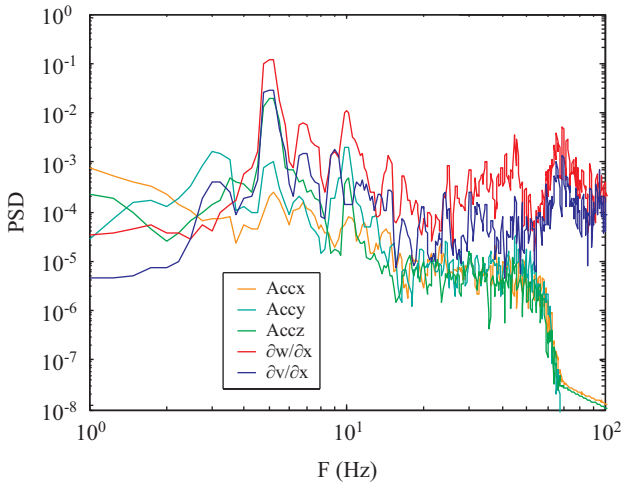

Fig. 3. The power spectra of the shear signal and the acceleration signal.

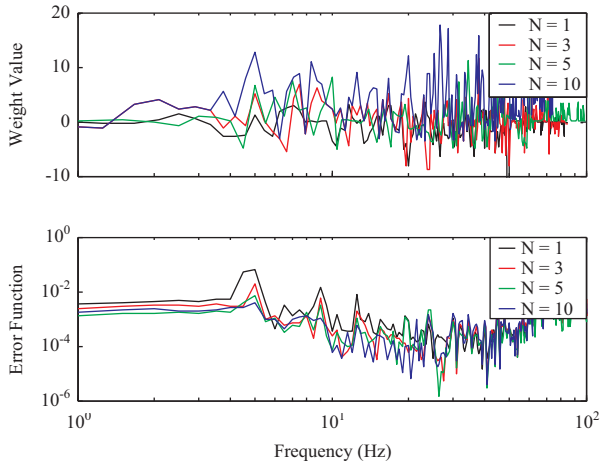

Fig. 4. Trajectory of the weight value and the error function in frequency domain.

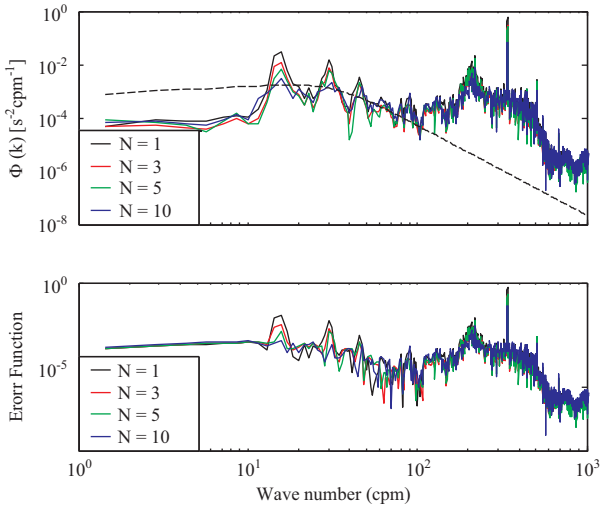

Fig. 5. Trajectory of the corrected spectrum and the error function in wavenumber domain.

which obscures the true environmental shear signal in the time domain (shown in Fig. 2).

The samples in Figs. 2(a) and (b) are the time series of the collected velocity shear. The instrument samples the time derivative of the shear probe signals, which are converted to the along-flow gradients of velocity ($\partial w/\partial x$, $\partial v/\partial x$) using the measured current speed for this record. The variation of the two perpendicular components $\partial w/\partial x$ and $\partial v/\partial x$ tracks closely, which indicates that the turbulence measured by the two shear probes is close to isotropic. Motions and vibrations of the observation instrument are revealed by the three-axis accelerometer records in Figs. 2 (c)-(e).

It is difficult to analyze the influence of the noise on the turbulence shear signals in the time domain. So, we transform the two kinds of signals into frequency domain and the frequency spectra can give considerable information on the quality of the data.

The power spectrum for each component of velocity shear is computed through a fast Fourier transform (FFT). In this paper, a FFT length of 4-s is chosen and each 3-min burst is segmented into half-overlapping 4-s-long portions for spectral analysis. Before calculating the frequency power spectra, each 4-s segment is detrended and Hanning windowed. The comparison between the shear frequency spectra and the accelerations frequency spectra is presented in Fig. 3.

The shear power spectra and acceleration spectra have high consistency near 5 Hz (vertical line). The main reason is that the turbulence instrument attached to the submerged buoy and the deployment lines of the rotor current meters take shape when fluid passes the line, which caused the Karman vortex street. The shedding of the vortex causes shaking of the mooring line and the turbulence instrument follows to shake, which makes interference for the measurement of the turbulence shear signals (Song et al., 2013). The shedding frequency can be computed using $f_{shedding} = 0.2U/D$, where $D = 0.01$ m is the diameter of the mooring line and U is the velocity of the instrument. In the segment processed in this paper, the corresponding velocity is about 0.26 m/s and the shedding frequency is calculated to be about 5 Hz. So, the high consistency of the power spectra at the shedding frequency indicates that the vibration of the instrument (represented as acceleration signals) seriously affects the measured shear signals.

The noise is removed with the improved turbulence denoising algorithm based on LMS adaptive filter described above. The adaptive trajectories of the weight value and the error function in frequency domain are presented in Fig. 4. The upper panel shows the change of the weight value and the lower panel shows the change of the error function obtained using Eq. (11), as the iteration number $N = 1, 3, 5, 10$ respectively. It is easy to find that with the increase of the iteration number, the weight value constantly adjusts until reaches to the optimal value, meanwhile, the obtained error function gradually decreases and eventually reaches to a steady value. The results prove that the improved turbulence denoising algorithm based on LMS adaptive filter

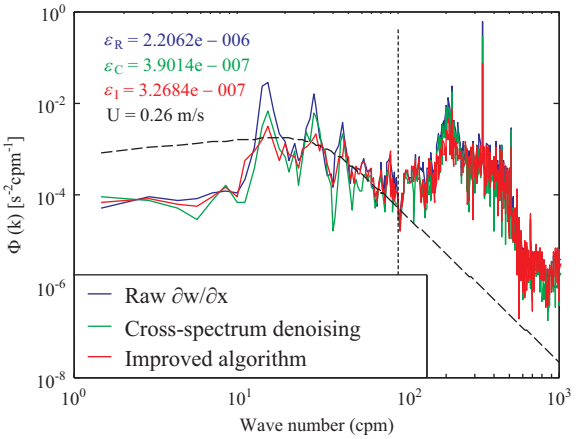

Fig. 6. The comparison of the raw spectrum , corrected spectrum and the Nasmyth theoretical spectrum.

is reliable and efficient.

To evaluate the validity of the improved denoising algorithm, the wavenumber power spectra are computed and compared with the Nasmyth theoretical spectrum. To observe the change of the wavenumber spectra with the increase of the iteration number, the wavenumber spectra and the error function in wavenumber domain are also presented in Fig. 5 at the iteration number N = 1, 3, 5, 10 respectively.

The cross-spectrum denoising algorithm is used as the comparison to evaluate the effectiveness of the improved denoising algorithm. The wavenumber spectra are integrated over a limited range of wavenumbers to calculate the dissipation rate of TKE (Eq. (13)). Here, we compare the corrected wavenumber spectrum using the improved denoising algorithm with the Nasmyth theoretical spectrum and the corrected wavenumber spectrum using the cross-spectrum denoising algorithm, which are shown in Fig. 6.

The above figure presents the denoising result of the improved turbulence denosing algorithm. The black dashed curve is the Nasmyth theoretical spectrum, and the other three solid curves are the observed spectra. Among the three curves, the blue curve is the raw signal spectrum, the red one is the spectrum after being corrected with the improved algorithm proposed in this paper and the green one shows the spectrum after being processed with cross-spectrum denoising algorithm. Compared with the cross-spectrum denoising algorithm, the observed spectrum corrected with the improved denoising algorithm based on LMS adaptive filter is fairly smooth between 15 and 40 cpm, which means the low wavenumber noise apparent in the raw spectrum is removed more effectively. Also, the spectrum shape agrees much more close with the Nasmyth theoretical spectrum up to 80 cpm. Furthermore, the dissipation rate of the TKE computed with the corrected shear signals using the improved denoising algorithm drops near an order of magnitude compared to the raw measured data, which provides reliable and effective data for the further analysis of the turbulence characteristics.

V. CONCLUSION

Based on the analysis of the characteristics of the vibration noise in the observed turbulence shear signals, an improved turbulence denoising algorithm based on LMS adaptive filtering is proposed in this work aiming at acquiring high-precision data. The algorithm takes the Nasmyth theoretical spectrum as the desired signal and conducts the adaptive weight value estimation for different wavenumbers, which improves the denoising effect. Compared with the traditional cross-spectrum denoising algorithm, the improved algorithm well improves the denoising effect at the shedding frequency. The sea data collected in the South China Sea with a moored instrument is used to verify the validity of the improved denoising algorithm. The results show that the improved denoising algorithm can reliably and effectively filter the turbulence vibration noise and supply effective turbulence signals to analyze the turbulence mixing characteristics.

ACKNOWLEDGEMENTS

This work was supported by the National High Technology Research and Development Program (“863”Program) of China under Grants No.2014AA093404 and No.2012AA090901, by the National Nature Science Foundation under Grant No. 61203070, and by the Nature Science Foundation of Shandong Province under Grant No. ZR2012DQ011.

REFERENCES

Song, D.-l., J.-J. Sun, B. Xue, Q.-L. Jiang and B.-W. Wu (2013). Mooring system of ocean turbulence observation based on submerged buoy. China Ocean Engineering 27(3), 369-378.

Dentino, M., J. Mccool and B. Widrow (1978). Adaptive filtering in the frequency domain. Proceedings of the IEEE 66(12), 1658-1659.

Deborah, M. D., J. Prasad, A. Aamina and A. R. Devi (2016). Phonocardiogram signal processing using lms adaptive algorithm. International Journal of Multidisciplinary Approach and Studies 03(2), 66-73.

Dixit, S. and D. Nagaria (2016). Design and analysis of cascaded lms adaptive filters for noise cancellation. Circuits Systems & Signal Processing, 1-25.

Fer, I. and M. B. Paskyabi (2013). Autonomous ocean turbulence measurements using shear probes on a moored instrument. Journal of Atmospheric and Oceanic Technology 31(2), 474-490.

Wolk, F., R. G. Lueck and L. St. Laurent (2009). Turbulence measurements from a glider. IEEE, 1-6.

Goodman, L., E. R. Levine and R. G. Lueck (2006). On measuring the terms of the turbulent kinetic energy budget from an AUV. Journal of Atmospheric and Oceanic Technology 23(7), 977-990.

Kalluri, S. and G. R. Arce (1999). A general class of nonlinear normalized adaptive filtering algorithms. IEEE Transactions on Signal Processing 47(8), 2262-2272.

Kang J.-J., H.-Q. Wu and Q.-X. Yang (2007). Ocean turbulence measurement technology. Ocean Technology 26(3), 19-23.

Levine, E. R. and R. G. Lueck (1999). Turbulence measurement from an autonomous underwater vehicle. Journal of Atmospheric and Oceanic Technology 16(11), 1533-1544.

Lueck, R. G., O. Hertzman and T. R. Osborn (1977). The spectral response of thermistors. Deep Sea Research Part II Topical Studies in Oceanography 24(10), 951-970.

Lueck, R. G. and D. Huang (1999). Dissipation measurement with a moored instrument in a swift tidal channel. Journal of Atmospheric and Oceanic

Technology 16(11), 1499-1505.

Lueck, R. G., D. Huang, D. Newman and J. Box (1997). Turbulence measurement with a moored instrument. Journal of Atmospheric and Oceanic Technology, 14(1), 143-161.

Lueck, R. G., F. Wolk, J. Hancyck and K. Black (2015). Hub-height time series measurements of velocity and dissipation of turbulence kinetic energy in a tidal channel. Current, Waves and Turbulence Measurement. IEEE.

Lueck, R. G., F. Wolk and H. Yamazaki (2002). Oceanic velocity microstructure measurements in the 20th century. Journal of Oceanography 58(1), 153-174.

Macoun, P. and R. Lueck (2004). Modeling the spatial response of the airfoil shear probe using different sized probes. Journal of Atmospheric and Oceanic Technology 21(2), 284-297.

Oakey, N. S. (1982). Determination of the rate of dissipation of turbulent energy from simultaneous temperature and velocity shear microstructure measurements. Journal of Physical Oceanography 12(3), 256-271.

Prandke, H. and A. Stips (1998). Microstructure profiler to study mixing and turbulent transport processes. Oceans IEEE, 179-183.

Paskyabi, M. B. and I. Fer (2013). Turbulence measurements in shallow water from a subsurface moored moving platform. Energy Procedia 35(35), 307-316.

Thomson, J., J. Talbert, A. De Klerk, S. Zippel, M. Guerra and L. Kilcher (2015). Turbulence measurements from moving platforms. Current, Waves and Turbulence Measurement (CWTM), 2015 IEEE/OES Eleventh, 1-5.

Widrow, B., J. R. Glover, J. M. Mccool and J. Kaunitz (1976). Adaptive noise cancelling: principles and applications. Proceedings of the IEEE 63(12), 1692-1716.

Wolk, F., H. Yamazaki, L. Seuront and R. G. Lueck (2002). A new free-fall profiler for measuring biophysical microstructure. Journal of Atmospheric and Oceanic Technology 19(5), 780-793.

Luan, X., X.-Y. Liu, H. Yang, S.-X. Wang, G.-J. Hou and D.-L. Song (2016). Characteristics of microstructure turbulence measurements with a moored instrument in the South China Sea. Marine Technology Society Journal 50(2), 54-62.

Zhang, Y.-Y., S.-M. Li, Y.-X. Hu, X.-X. Jiang and H. D. Guo (2013). Improvement of LMS method and its application combined with EEMD in vehicle vibration signal denoising. Journal of Vibration and Shock 32(20), 61-66.